

The Production and Decay of Tau Leptons in e^+e^- Annihilation at PETRA Energies

TASSO Collaboration

M. Althoff, W. Braunschweig, F.J. Kirschfink, K. Lübelmeyer, H.-U. Martyn, P. Roskamp,
D. Schmitz, H. Siebke, W. Wallraff

I. Physikalisches Institut der RWTH, D-5100 Aachen, Federal Republic of Germany^a

J. Eisenmann, H.M. Fischer, H. Hartmann, A. Jocksch, G. Knop, H. Kolanoski, H. Kück
V. Mertens, R. Wedemeyer

Physikalisches Institut der Universität, D-5300 Bonn, Federal Republic of Germany^a

B. Foster

H.H. Wills Physics Laboratory, University of Bristol, Bristol BS8 1TL, UK^b

A. Eskreys¹, K. Gather, M. Hildebrandt, H. Hultschig, P. Joos, U. Kötz, H. Kowalski, A. Ladage,
B. Löhr, D. Lüke, P. Mättig, D. Notz, R.J. Nowak², J. Pyrlík, E. Ronat³, M. Rushton, W. Schütte,
D. Trines, T. Tymieniecka², G. Wolf, G. Yekutieli³, Ch. Xiao⁶

Deutsches Elektronen-Synchrotron DESY, D-2000 Hamburg 50, Federal Republic of Germany^a

R. Fohrmann, E. Hilger, T. Kracht, H.L. Krasemann, P. Leu, E. Lohrmann, D. Pandoulas, G. Poelz,
K.U. Pösnecker, B.H. Wiik

II. Institut für Experimentalphysik der Universität, D-2000 Hamburg, Federal Republic of Germany^a

R. Beuselinck, D.M. Binnie, A.J. Campbell⁴, P.J. Dornan, D.A. Garbutt, C. Jenkins, T.D. Jones,
W.G. Jones, J. McCardle, J.K. Sedgbeer, J. Thomas, W.A.T. Wan Abdullah⁷

Department of Physics, Imperial College, London SW7 2BZ, UK^b

K.W. Bell⁸, M.G. Bowler, P. Bull, R.J. Cashmore, P.E.L. Clarke, P. Dauncey, R. Devenish,
P. Grossmann, C.M. Hawkes, S.L. Lloyd, D.J. Mellor, C. Youngman

Department of Nuclear Physics, University, Oxford OX1 3RH, UK^b

G.E. Forden, J.C. Hart, J. Harvey, D.K. Hasell, D.H. Saxon, P.L. Woodworth⁵

Rutherford Appleton Laboratory, Chilton, Didcot, Oxon OX11 0QX, UK^b

F. Barreiro, S. Brandt, M. Dittmar, M. Holder, G. Kreutz, B. Neumann

Fachbereich Physik der Universität-Gesamthochschule, D-5900 Siegen, Federal Republic of Germany^a

E. Duchovni, Y. Eisenberg, U. Karshon, G. Mikenberg, R. Mir, D. Revel, A. Shapira

Weizmann Institute, Rehovot, Israel^c

G. Baranko, A. Caldwell, M. Cherney, J. M. Izen, M. Mermikides, S. Ritz, G. Rudolph, D. Strom,
M. Takashima, H. Venkataramania, E. Wicklund, Sau Lan Wu, G. Zobernig

Department of Physics, University of Wisconsin, Madison, WI 53706, USA^d

Received 20 September 1984

¹ On leave from Institute of Nuclear Physics, Cracow, Poland

² On leave from Warsaw University, Poland

³ On leave from Weizmann Institute, Rehovot, Israel

⁴ Now at University of Glasgow, UK

⁵ Now at Institute of Oceanographic Sciences, Bidston, Merseyside, UK

⁶ Now at University of Science and Technology of China, Hefei

⁷ On leave from Universiti Malaya, Kuala Lumpur

⁸ On leave from Rutherford Appleton Laboratory, Chilton, UK

^a Supported by the Deutsches Bundesministerium für Forschung und Technologie

^b Supported by the UK Science and Engineering Research Council

^c Supported by the Minerva Gesellschaft für Forschung mbH

^d Supported by the US Department of Energy contract DE-AC02-76R00881

Abstract. We have observed τ pair production at average CM energies of 13.9, 22.3, 34.5 and 43.1 GeV. The cross-sections are consistent with QED, the cut off parameters being $\Lambda_+ > 161$ GeV and $\Lambda_- > 169$ GeV (95% CL). The topological branching fraction of the τ to 1 charged particle, B_1 , is 0.847 ± 0.011 (stat) $^{+0.016}_{-0.013}$ (syst) and no decays to 5 charged particles were observed resulting in $B_5 < 0.007$ (95% CL). Within the 3 charged track final state $B(\tau^- \rightarrow \pi^- \pi^+ \pi^- \nu) / (B(\tau^- \rightarrow \pi^- \pi^+ \pi^- \nu) + B(\tau^- \rightarrow \pi^- \pi^+ \pi^- \pi^0 \nu)) = 0.37 \pm 0.35$

In this paper we report measurements of the reaction $e^+e^- \rightarrow \tau^+\tau^-$ at an average CM energy of $W = 34.5$ GeV, based on an integrated luminosity of 69.4 pb^{-1} . The tau decay branching fractions, the total cross section and the forward-backward asymmetry for tau pair production are determined. The measurement of the topological branching fractions B_1, B_3 and B_5 , where the τ decays to one, three or five stable charged particles with or without neutrals, is of particular interest as there have recently been substantial changes in the measured values [1]. We also present measurements of the total cross

section for $e^+e^- \rightarrow \tau^+\tau^-$ at mean CM energies of $W = 13.9, 22.3$ and 43.1 GeV based on integrated luminosities of $1.8, 3.2$ and 13.0 pb^{-1} respectively. At these energies the event sample is substantially smaller and we have therefore concentrated on the 34.5 GeV data for which we describe the analysis in detail.

The experiment was performed at the electron-positron storage ring, PETRA, with the TASSO detector, which has been described in detail elsewhere [2]. In this analysis particular use was made of the event topology and of the electron, photon and muon detection systems. The event topology was determined from the charged tracks reconstructed in the proportional and drift chambers [3] of the central detector. Electrons and photons were identified using the two different types of electromagnetic calorimeter; the liquid argon barrel calorimeter [4] (LABC) and the hadron arm shower counters [5] (HASC) with geometrical acceptances of 40% and 18% of the solid angle. Muons were identified by their ability to penetrate the electromagnetic calorimeters and iron absorber and to give hits in the muon proportional chambers [6] (MUCH) behind the absorber. The muon chambers cover 43% of 4π , and the overlap between the muon chambers and electromagnetic calorimeters is 27% of 4π .

Table 1. Lone track identification (a) before and (b) after background subtraction. Regions with no muon chamber coverage are denoted by MUCH. Entries marked – denote regions not used or not applicable. In part (b) the (1–1) channels $e-e$ and $\mu-\mu$ were omitted due to severe background (see text)

| Detector region: | LABC. MUCH | LABC. MUCH | HASC. MUCH | HASC. MUCH | MUCH only |
|--|------------|------------|------------|------------|-----------|
| (a) Number of events before background subtraction | | | | | |
| 1–1 | | | | | |
| $\mu-\mu$ | 132 | – | 73 | – | – |
| $\mu-e$ | 10 | – | 9 | – | – |
| $\mu-h$ | 48 | – | 26 | – | – |
| $e-e$ | 24 | – | 19 | – | – |
| $e-h$ | 38 | – | 29 | – | – |
| $h-h$ | 44 | – | 18 | – | – |
| 1–3 | | | | | |
| $\mu-3$ | 5 | – | 13 | – | 6 |
| $e-3$ | 17 | 18 | 9 | 1 | – |
| $h-3$ | 30 | 50 | 24 | 16 | – |
| (b) Number of events after background subtraction | | | | | |
| 1–1 | | | | | |
| $\mu-e$ | 9.9 | – | 8.9 | – | – |
| $\mu-h$ | 32.6 | – | 19.9 | – | – |
| $e-h$ | 23.7 | – | 22.8 | – | – |
| $h-h$ | 34.4 | – | 16.8 | – | – |
| 1–3 | | | | | |
| $\mu-3$ | 4.8 | – | 12.5 | – | 5.8 |
| $e-3$ | 15.4 | 16.5 | 7.8 | 0.9 | – |
| $h-3$ | 27.3 | 47.3 | 22.5 | 15.5 | – |

Table 2. Particle feed through and identification probabilities for different regions of the detector

| Particle type as identified by the detector | Original particle type | | | |
|---|------------------------|-------------------|-----------------|-----------------|
| | μ | e | h | |
| LABC. MUCH | μ | 0.933 ± 0.002 | 0.00 ± 0.00 | 0.02 ± 0.01 |
| | e | 0.000 ± 0.000 | 0.84 ± 0.02 | 0.01 ± 0.01 |
| | h | 0.067 ± 0.002 | 0.15 ± 0.02 | 0.93 ± 0.02 |
| LABC. MUCH | μ | — | — | — |
| | e | 0.000 ± 0.000 | 0.84 ± 0.02 | 0.01 ± 0.01 |
| | h | 1.000 ± 0.000 | 0.15 ± 0.02 | 0.95 ± 0.01 |
| HASC. MUCH | μ | 0.947 ± 0.002 | 0.00 ± 0.00 | 0.02 ± 0.01 |
| | e | 0.000 ± 0.000 | 0.77^a | 0.04^a |
| | h | 0.053 ± 0.002 | 0.23^a | 0.91^a |
| HASC. MUCH | μ | — | — | — |
| | e | 0.000 ± 0.000 | 0.77^a | 0.04^a |
| | h | 1.000 ± 0.000 | 0.23^a | 0.93^a |
| MUCH | μ | 0.940 ± 0.002 | 0.00 ± 0.00 | 0.02 ± 0.01 |
| | e | — | — | — |
| | h | — | — | — |

The total calculated feedthrough for any given particle does not necessarily sum to unity due to some tracks not having associated energy clusters

^a In this analysis electrons and hadrons were separated in the LABC region only (see text)

Event Selection

The number of charged tracks observed in the central detector was used to select four categories of events: one track recoiling against another (1–1), one against three (1–3), three against three (3–3) and one against five (1–5). The categories (3–5) and (5–5) were not considered due to their low rate from tau pair production and the large backgrounds from hadronic events. The event selection requirements are described in detail in Appendix A. Two types of cut were used, the first selecting the required topology and the second reducing background. These cuts resulted in a total of 470 (1–1), 350 (1–3) and 36 (3–3) events. No candidates for the topology (1–5) were found.

The events of categories (1–1) and (1–3) were subdivided according to the identity of the lone track as described in Appendix B if the lone track was inside the particle identification acceptance of the electromagnetic calorimeters and/or the muon chambers. The results of these classification procedures are shown in Table 1a. Whenever at least 2 tracks in a 3-track τ decay (1–3 and 3–3 categories) entered the LABC then the 3-tracks were divided into 2 categories depending upon whether or not there were neutral energy clusters within 45° of any of the charged tracks. The numbers of 3-track systems falling into these classes were 62 and 41

respectively. A neutral energy cluster was defined as a calorimeter deposit of >200 MeV which was not associated with any charged track.

The efficiencies and misidentification probabilities for the particle identification criteria are shown in Table 2. For all but hadrons these probabilities were determined from data. The electron identification probabilities were determined using the reaction $e^+e^- \rightarrow e^+e^-$ at beam energies of 7, 11 and 17 GeV and at lower momentum in the LABC region, using $e^+e^- \rightarrow e^+e^-e^+e^-$ events. The muon identification probabilities were determined from $e^+e^- \rightarrow \mu^+\mu^-$ events at 7, 11 and 17 GeV. The probability for hadron identifications was determined using the Monte Carlo program GEISHA [13] to simulate hadronic showers. It is clear from Table 2 that the contamination (feed through) of any lone track channel resulting from the other channels is relatively small.

Background Calculations

The e^+e^- and $\mu^+\mu^-$ classes in the (1–1) category contained large contaminations from the reactions $e^+e^- \rightarrow e^+e^-$ and $e^+e^- \rightarrow \mu^+\mu^-$. These channels were therefore excluded in the subsequent analysis. The residual contamination of other classes in the (1–1) category resulting from misidentification of $e^+e^- \rightarrow e^+e^-$ and $e^+e^- \rightarrow \mu^+\mu^-$ were removed by scanning. The contamination of the (1–3) and (3–3) categories from e^+e^- events containing a radiated photon was estimated by searching for 3-track systems containing an identified electron. The background in the (1–3) category was found to be $3.2 \pm 1.6\%$. The contamination in the (3–3) category from e^+e^- events was negligible.

The contamination of the (1–3), (3–3) categories from (1–1), (1–3) events with associated interactions in the material of the detector was estimated by Monte Carlo techniques to be $1.3 \pm 0.3\%$ and $2.5\% \pm 0.6\%$, respectively.

The contamination resulting from two-photon induced $\tau^+\tau^-$ production was estimated using Monte Carlo techniques [7]. A background of $\sim 2\%$ independent of event category was found. The backgrounds from two-photon induced hadron production [8] were estimated in a similar way, and were found to be negligible.

To estimate the contamination from $e^+e^- \rightarrow$ hadrons in the (1–3) and (3–3) topologies the selection of the (3–3) sample was repeated without making a 3-track effective mass cut of 2.0 GeV (see Appendix A cut (3h)). The number of events where at least one of the 3-track masses was greater than 2.0 GeV was then used to normalise the Monte Car-

Table 3. Number of events in raw, background and final background subtracted event samples. Errors include statistical and background contributions

| | | Raw Data | Background Process | | | | | Final Data | |
|--|---------|----------|-----------------------------|---------------------------------|--|--|--|------------|-------------------------------------|
| | | | $e^+e^- \rightarrow e^+e^-$ | $e^+e^- \rightarrow \mu^+\mu^-$ | $11 \rightarrow 13$ $13 \rightarrow 33$ | $e^+e^- \rightarrow e^+e^- \tau^+\tau^-$ | $e^+e^- \rightarrow e^+e^- + \text{hadrons}$ | | $e^+e^- \rightarrow \text{hadrons}$ |
| Sample with lone track identified: | | | | | | | | | |
| LABC. | $\mu-e$ | 10 | 0.0 | 0.0 | | 0.1 | 0.0 | 0.0 | 9.9 ± 3.2 |
| MUCH | $\mu-h$ | 48 | 0.0 | 15.0 | | 0.4 | 0.0 | 0.0 | 32.6 ± 6.5 |
| | $e-h$ | 38 | 14.0 | 0.0 | – | 0.3 | 0.0 | 0.0 | 23.7 ± 5.7 |
| | $h-h$ | 44 | 4.0 | 5.0 | | 0.6 | 0.0 | 0.0 | 34.4 ± 6.5 |
| HASC. | $\mu-e$ | 9 | 0.0 | 0.0 | | 0.1 | 0.0 | 0.0 | 8.9 ± 3.0 |
| MUCH | $\mu-h$ | 26 | 0.0 | 6.0 | | 0.1 | 0.0 | 0.0 | 19.9 ± 4.7 |
| | $e-h$ | 29 | 6.0 | 0.0 | – | 0.2 | 0.0 | 0.0 | 22.8 ± 5.0 |
| | $h-h$ | 18 | 1.0 | 0.0 | | 0.2 | 0.0 | 0.0 | 16.8 ± 4.1 |
| LABC | $e-3$ | 35 | 2.0 | 0.0 | 0.5 | 0.6 | 0.0 | 0.0 | 31.9 ± 5.7 |
| | $h-3$ | 80 | 1.0 | 0.0 | 1.0 | 1.5 | 1.1 | 0.8 | 74.6 ± 8.9 |
| HASC | $e-3$ | 10 | 1.0 | 0.0 | 0.1 | 0.2 | 0.0 | 0.0 | 8.7 ± 3.0 |
| | $h-3$ | 40 | 0.0 | 0.0 | 0.5 | 0.6 | 0.5 | 0.4 | 38.0 ± 6.3 |
| MUCH | $\mu-3$ | 24 | 0.0 | 0.0 | 0.3 | 0.6 | 0.0 | 0.0 | 23.1 ± 4.9 |
| Topological sample (1–1 excludes $\mu-\mu$ and $e-e$) | | | | | | | | | |
| | 1–1 | 222 | 25.0 | 26.0 | – | 2.0 | 0.0 | 0.0 | 169.0 ± 14.0 |
| | 1–3 | 350 | 11.3 | 0.0 | 4.6 | 5.6 | 2.0 | 2.0 | 324.5 ± 19.4 |
| | 3–3 | 36 | 0.0 | 0.0 | 0.8 | 0.4 | 1.0 | 1.0 | 32.8 ± 6.0 |

lo [9] prediction for the hadronic background to the (3–3) topology and was found to be $3.0 \pm 3.0\%$. Using this normalisation the contamination of the (1–3) category was found to be $0.6 \pm 0.6\%$.

The backgrounds in the various event categories are shown in Table 3. The results of background corrections to the lone track categories are shown in Table 1b.

Acceptance Calculations

The acceptances for the reaction $e^+e^- \rightarrow \tau^+\tau^-$ were determined for combinations of the possible τ decay modes [10], i.e. lone track ($\tau^- \rightarrow e^- \nu \bar{\nu}$, $\mu^- \nu \bar{\nu}$, $\pi^- \nu$, $\pi^- \pi^0 \nu$, $\pi^- \pi^0 \pi^0 \nu$, $\pi^- \pi^0 \pi^0 \pi^0 \nu$), 3-track ($\tau^- \rightarrow \pi^- \pi^+ \pi^- \nu$, $\pi^- \pi^+ \pi^- \pi^0 \nu$) and 5-track ($\tau^- \rightarrow \pi^- \pi^+ \pi^- \pi^+ \pi^- \nu$) using an $e^+e^- \rightarrow \tau^+\tau^-$ event generator [11] which included higher order QED corrections and simulated the response of the detector. The generated events were passed through the same data reduction and track finding procedures as applied to the data.

The trigger efficiencies were determined from events in the data satisfying more than one independent trigger. The trigger efficiency for the (1–1) category was found to be $93.7\% \pm 0.2\%$ averaged over the whole 34.5 GeV data sample. This corre-

sponds to trigger efficiencies of $96.8\% \pm 0.1\%$ and $99.9\% \pm 0.1\%$ for the (1–3) and (3–3) categories. The efficiency of the track and timing cuts was found to be $96.8\% \pm 0.2\%$ for the (1–1) category and was 100% for the (1–3) and (3–3) categories.

Corrections arising from the calorimeter total energy cut (Appendix A cut (1g)) in the (1–1) selection were calculated using the (1–3) category where the lone track entered the calorimeter acceptance. The energy deposited by (1–1) events was estimated by combining lone tracks from different (1–3) events. Losses of events of the type $e-h$ and $h-h$ were found to be $10\% \pm 5\%$. Losses in the remaining channels were negligible.

Luminosity

The luminosity used in this analysis was measured [12] using Bhabha scattering events recorded in the small angle luminosity monitors, and the central detector tracking chambers. The luminosities obtained by the two methods were in good agreement throughout the entire running period and the integrated luminosities of 1.8, 3.2, 69.4 and 13.0 pb^{-1} represent the average of these measurements at $W = 13.9, 22.3, 34.5$ and 43.1 GeV respectively. The as-

sociated systematic errors were 5.0%, 5.0%, 3.0% and 4.0% respectively.

Results

(i) 5-Track Branching Fraction

We observed no events in the (1–5) category. We used this result to set a limit on $\sigma_{\tau\tau} B_1 B_5$. Assuming the QED cross-section for $\tau^+ \tau^-$ production, a lone track branching fraction $B_1 = 0.85$ (see below) and a 5-track final state containing only five charged pions and a neutrino, we obtain an upper limit for $B_5 < 0.007$ with 95% confidence. In the following analysis $B_5 = 0$ was assumed.

(ii) Composition of the 3-Track System

Since B_5 is negligible the contribution to B_3 from decays of the type $\tau^- \rightarrow \pi^- \pi^+ \pi^- \pi^0 \pi^0 \nu$ is also presumably small. Taking this contribution to be zero and using the 62 and 41 3-track systems with and without neutral energy clusters in the LABC, the ratio $F = B(\tau^- \rightarrow \pi^- \pi^+ \pi^- \nu) / (B(\tau^- \rightarrow \pi^- \pi^+ \pi^- \nu) + B(\tau^- \rightarrow \pi^- \pi^+ \pi^- \pi^0 \nu))$ was determined. Monte Carlo [13] events of the type $\tau^- \rightarrow \pi^- \pi^+ \pi^- \nu (\pi^- \pi^+ \pi^- \pi^0 \nu)$ were generated and passed through the detector simulation, 50% (68%) had neutral energy clusters within 45° of any of the charged tracks. Correcting for the relative acceptance of the two decay modes we find $F = 0.37^{+0.35}_{-0.20}$. Using this value of F the acceptances were then calculated for the topological event categories involving 3-track decays of the τ .

(iii) Total Cross Section

and 1 and 3 Track Branching Fractions at 34.5 GeV

The $\tau^+ \tau^-$ cross section, $\sigma_{\tau\tau}$, the lone track branching fractions into electron (B_e), muon (B_μ) and hadron (B_h) and the topological branching fractions B_1 and B_3 were determined. To obtain the acceptances of the (1–1) and (1–3) categories we assumed the composition of the lone track hadronic system to be $\pi^- : \pi^- \pi^0 : \pi^- \pi^0 \pi^0 : \pi^- \pi^0 \pi^0 \pi^0 = 24:44:12:20$ [1]. Changes in the acceptance due to uncertainties in these ratios were included in the systematic errors.

A fit was made to the number of events in the categories (1–1), (1–3) and (3–3) and to the number of events with identified lone track systems as given in Table 1b. In the fit electrons and hadrons were only separated in the LABC region, where the detailed shower information allows reliable identification. The chisquare, $\chi^2 = \sum_{i,j} (N_{ij} - E_{ij})^2 / (E_{ij} + B_{ij})$,

was minimised where N_{ij} are the number of events of type $i-j$ seen in the data, E_{ij} are the expected number of events and B_{ij} is the square of the error on

the background. The expected number of events E_{ij} contained contributions from those final states where i and j were correctly identified and those where i and/or j result from misidentification. The fit parameters (the τ decay branching fractions and total cross section, $\sigma_{\tau\tau}$) have been determined ($\chi^2 = 6.3/7$ df) to be

$$B_\mu = 0.129 \pm 0.017 (\text{stat}) \pm 0.007 (\text{syst})$$

$$B_e = 0.204 \pm 0.030 \quad \begin{matrix} +0.014 \\ -0.009 \end{matrix}$$

$$B_h = 0.515 \pm 0.029 \quad \begin{matrix} +0.016 \\ -0.026 \end{matrix}$$

giving

$$B_1 = B_\mu + B_e + B_h = 0.847 \pm 0.011 \pm 0.016$$

$$B_3 = 1 - B_1 = 0.153 \pm 0.011 \pm 0.013$$

and a total cross section of

$$\sigma_{\tau\tau} = 0.075 \pm 0.004 (\text{stat}) \pm 0.005 (\text{syst}) \text{ nb}$$

corresponding to

$$\frac{\sigma_{\tau\tau}}{\sigma_{\text{QED}}} = 1.03 \pm 0.05 (\text{stat}) \pm 0.06 (\text{syst})$$

where the results were corrected for unseen K_L^0 decays (a 0.4% contribution to $\sigma_{\tau\tau}$). No evidence was found to suggest that the somewhat low value of B_μ was due to the detector or the analysis used. We have repeated the fit using the world averages [1] of $B_e = 0.171$ and $B_\mu = 0.176$. The χ^2 for the fit was 13.9/9df resulting in $B_1 = 0.846 \pm 0.011 (\text{stat}) \pm 0.013 (\text{syst})$, $B_3 = 0.154 \pm 0.011 (\text{stat}) \pm 0.013 (\text{syst})$ and $\sigma_{\tau\tau}/\sigma_{\text{QED}} = 1.02 \pm 0.05 (\text{stat}) \pm 0.11 (\text{syst})$. The values of B_1 and $\sigma_{\tau\tau}$ are consistent for both fits and are in good agreement with other recent publications [1].

The systematic errors on $\sigma_{\tau\tau}$ and B_1 were obtained by (1) varying the composition of the lone track hadronic system (resulting in changes of +0.04 – 0.10, +0.002 – 0.008 to $\sigma_{\tau\tau}/\sigma_{\text{QED}}$, B_1 respectively), (2) varying the composition of the 3-track system using the error on the determination of F (± 0.03 , +0.014 – 0.010), (3) changing the LABC feed-through probabilities within the measured errors (0,0), (4) including the uncertainties from other selection cuts (+0.02 – 0.03, +0.007 – 0.003) and (5) making allowance for systematic errors in the radiative correction (± 0.02 , 0.0) and the luminosity measurement (± 0.03 , 0.0). The final systematic errors were obtained by adding these in quadrature.

(iv) Total Cross Sections at 13.9, 22.3 and 43.1 GeV

To obtain the cross section for tau pair production at the energies $W = 13.9, 22.3$ and 43.1 GeV we have used only the (1–3) category. We observe 63, 46

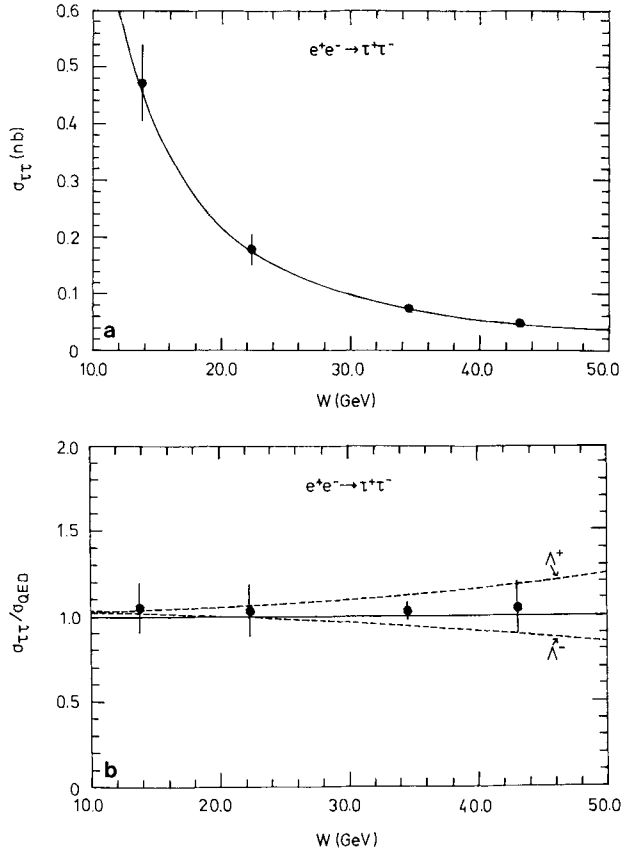


Fig. 1. **a** Measured tau pair cross section (nb). The solid curve shows the lowest order QED prediction. **b** Normalised tau pair cross section, $\sigma_{\tau\tau}/\sigma_{\text{QED}}$. The 95% confidence level limits on Λ_{\pm} (dashed curve) are shown, where the overall normalisation was allowed to vary within the systematic error

and 46 events of this category at the three energies respectively. Event selection, background subtraction, radiative corrections, acceptance corrections and trigger efficiencies were calculated as described above. Using our measured values of $B_1 B_3$ above $\sigma_{\tau\tau}$ is determined to be 0.47 ± 0.06 , 0.18 ± 0.03 and 0.049 ± 0.008 nb respectively. The results shown in Fig. 1 are in good agreement with QED and with other recent measurements [14].

In a previous publication [15] $B_1 B_3 = 0.19$ was used together with the then existing τ decay branching fractions. In this analysis the use of all decay categories and improved knowledge of τ decays involving π^0 's allows a better calculation of the cross section.

The W -dependence of the cross section was used to determine the τ cut off parameters, Λ_+ and Λ_- , defined by

$$\sigma_{\tau\tau} = \sigma_{\text{QED}} [1 \mp W^2 / (W^2 - \Lambda_{\pm}^2)]^2$$

Fits to the cross sections, allowing the overall normalisation to vary within the systematic error, yield-

ed the following bounds at 95% confidence level, $\Lambda_+ > 161$ GeV and $\Lambda_- > 169$ GeV as shown in Fig. 1.

(v) Asymmetry Measurements at 34.5 GeV and τ Neutral Current Couplings

The tau pair events were used to measure the weak neutral current couplings of the tau lepton. Contributions from electromagnetic and weak neutral currents lead to a differential cross section for $\tau^+ \tau^-$ production of the form [16, 17]:

$$\begin{aligned} \frac{d\sigma}{d\Omega} = \frac{\alpha^2}{4W^2} \{ & (1 + \cos^2 \theta)(1 + 2g_v^e g_v^\tau \text{Re}(\chi)) \\ & + (g_v^{e^2} + g_a^{e^2})(g_v^{\tau^2} + g_a^{\tau^2})|\chi|^2 \\ & + 4\cos \theta (g_a^e g_a^\tau \text{Re}(\chi) + 2g_v^e g_v^\tau g_a^e g_a^\tau |\chi|^2) \} \end{aligned} \quad (2)$$

where $\chi = \frac{G_F M_z^2}{2\sqrt{2}\pi\alpha} \frac{W^2}{(W^2 - M_z^2 + iM_z\Gamma_z)}$ is the weak neutral current pole term with mass M_z and width Γ_z , θ is the scattering angle measured between the incoming e^+ and outgoing τ^+ and g_v and g_a are the vector and axial vector coupling constants. The presence of a weak neutral current can produce changes in the cross section ($\sim g_v^e g_v^\tau$) and introduce a forward-backward asymmetry ($\sim g_a^e g_a^\tau$). The most prominent effect at our energies is the forward-backward asymmetry.

The differential cross section of (2) has the general form:

$$\frac{d\sigma}{d\Omega} = b_0(1 + b_1 \cos \theta + \cos^2 \theta) \quad (3)$$

where we define θ by $\cos \theta = \mathbf{e}^+ \cdot (\boldsymbol{\tau}^+ - \boldsymbol{\tau}^-) / |\mathbf{e}^+| |\boldsymbol{\tau}^+ - \boldsymbol{\tau}^-|$, with \mathbf{e}^+ being the momentum vector of the incident positron and $\boldsymbol{\tau}^+$ and $\boldsymbol{\tau}^-$ being the summed momentum vectors of the outgoing charged decay products of the tau. Figure 2 shows the differential cross section at $W = 34.5$ GeV after applying corrections for acceptances, QED radiative effects [18] and backgrounds. The dashed curve corresponds to the $1 + \cos^2 \theta$ form expected from lowest order QED. To quantify any forward-backward asymmetry two approaches have been used:

(a) The direct asymmetry was determined by counting the number of events with $0.8 > \cos \theta > 0$ (F) and $0 > \cos \theta > -0.8$ (B) and forming

$$A_{\text{dir}}(|\cos \theta| < 0.8) = \frac{F - B}{F + B}$$

Higher order QED processes [17] lead to a radiative correction to A_{dir} of 0.007 ± 0.005 , higher order cor-

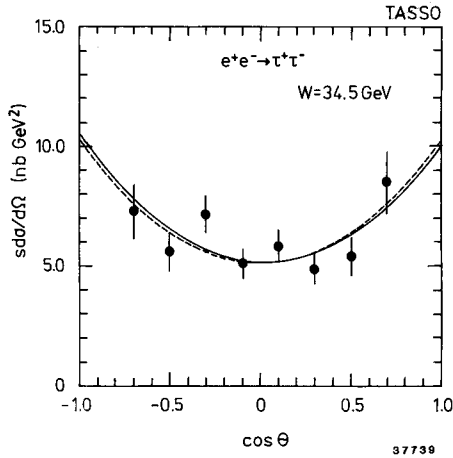


Fig. 2. The measured tau pair differential cross section at $W = 34.5$ GeV. The dashed line has the form $(1 + \cos^2 \theta)$ expected from lowest order QED, normalised to the data and the full line is the result of the fit

rections to the weak current are ~ 0.006 [19] and are not applied. The corrected asymmetry was found to be $A_{\text{dir}}(|\cos \theta| < 1) = -0.048 \pm 0.043$.

(b) The angular distribution was fitted using (3) and the asymmetry, A , for the entire range determined from $A(|\cos \theta| < 1) = \frac{2}{3} b_1$. The results of the fit are shown in Fig. 2 by the solid curve. The asymmetry determined was $A(|\cos \theta| < 1) = -0.049 \pm 0.053^{+0.013}_{-0.012}$. This result is consistent with the GWS prediction of -0.092 ($\sin^2 \theta_w = 0.228$ [20], $M_z = 93$ GeV [21]).

The asymmetry was used to calculate g_a^e using the expression derived from (2) i.e.,

$$A = -2.7 \cdot 10^{-4} \cdot g_a^e g_a^{\tau} \frac{W^2}{(1 - W^2/M_z^2)}$$

where we assume $M_z = 93$ GeV and $g_a^e = -0.514 \pm 0.058$ [22]. The value obtained, $g_a^e = -0.26 \pm 0.34$, is consistent with the GWS model and with other measurements [1, 14].

Conclusions

We have used the distinctive topology of tau pair final states to select event samples of the 1–3 and 3–3 topologies and have used the particle identification properties of the TASSO detector to select a sample of 1–1 topology events. No events of the 1–5 topology were found, resulting in an upper limit for the 5-track topological branching fraction, B_5 , where the τ decays to 5 stable charged particles of $B_5 < 0.007$ (95% CL). In the 3-track sample the π^0 composition was found to be $F = B(\tau^- \rightarrow \pi^- \pi^+ \pi^- \nu) / (B(\tau^- \rightarrow \pi^- \pi^+ \pi^- \nu) + B(\tau^- \rightarrow \pi^- \pi^+ \pi^- \pi^0 \nu)) = 0.37^{+0.35}_{-0.20}$, under the assumption that $B(\tau^- \rightarrow \pi^- \pi^+ \pi^- \pi^0 \nu)$

$= 0$. The event samples have been used to calculate the topological branching fractions B_1 and B_3 . Assuming $B_5 = 0$ we find $B_1 = 0.847 \pm 0.011$ (stat) $^{+0.016}_{-0.013}$ (syst), giving $B_3 = 1 - B_1 = 0.153 \pm 0.011$ (stat) $^{+0.013}_{-0.016}$ (syst) confirming recent results [1]. The total production cross section has been found to agree with that expected from QED for pointlike spin 1/2 particles, leading to cut off parameters of $A_+ > 161$ GeV and $A_- > 169$ GeV (95% CL). The differential cross section for tau pair production has been used to determine the forward-backward asymmetry A . We find $A(|\cos \theta| < 1) = -0.049 \pm 0.053^{+0.013}_{-0.012}$.

Acknowledgements. We thank the DESY directorate for their continuing support of the experiment and the PETRA machine group for their tremendous efforts. We thank the staff of the DESY Rechenzentrum, of the Rutherford Appleton Laboratory Computer Centre and the HEP computers of the Oxford Nuclear Physics Laboratory. Those of us from abroad wish to thank the DESY directorate for the hospitality extended to us while working at DESY.

Appendix A. Event Selection Requirements

In this appendix we describe the selection criteria in searching for the various τ topological samples.

Topology (1–1)

To be considered as a candidate (1–1) event the following cuts had to be satisfied:

(1a) exactly two reconstructed charged tracks should be seen in the event, where each track satisfied: (i) $d_0 < 0.4$ cm, (ii) $|z| < 10.0$ cm, (iii) $-3 \text{ ns} < t_{\text{meas}} - t_{\text{pred}} < 2 \text{ ns}$ and (iv) $p > 2$ GeV/c, where d_0 is the radial distance of the track from the beam line at its point of closest approach (the resolution of the measured position of the beam line, determined from Bhabha scattering events, was 0.1 mm and the d_0 resolution was 0.15 mm), z is the distance along the beam line from the interaction point to the point at which d_0 was measured, t_{meas} is the measured time of flight to the inner time-of-flight counters, t_{pred} that calculated using the measured path length and assuming the particle to be travelling at the velocity of light, and p is the measured track momentum,

(1b) the difference in the measured time of flight of the two tracks, t_1 and t_2 , satisfied $|t_1 - t_2| < 5.0$ ns,

(1c) the event satisfied the coplanarity trigger, which required that at least two tracks back to back within 27° in the plane perpendicular to the beam line,

(1d) the summed charge satisfied $\sum Q = 0$,

(1e) the opening angle, α_{12} , between the two tracks satisfied $120^\circ < \alpha_{12} < 178^\circ$,

(1f) each track was projected to enter the MUCH and also the LABC or HASC acceptance,

(1g) the total electromagnetic shower energy, E_{cal} , deposited in the calorimeters satisfied $E_{\text{cal}} < 20$ GeV and

(1h) the summed transverse momentum relative to the beam line satisfied $|\sum p_{xy}| > 0.5$ GeV/c.

Cut (1e) reduces $e^+e^- \rightarrow e^+e^-$ and $e^+e^- \rightarrow \mu^+\mu^-$ backgrounds, (1g) $e^+e^- \rightarrow e^+e^-$ and (1h) $e^+e^- \rightarrow e^+e^-e^+e^-$ and $e^+e^- \rightarrow e^+e^-\mu^+\mu^-$ backgrounds. Events which satisfied all these cuts, except for having additional tracks failing the track requirements of (1a) (i.e. not originating from the interaction point), were scanned to find those where these extra tracks were due to back-scattering in the coil (back-scattering is not accounted for in our detector simulation program). Five events were found by scanning, which were retained, resulting in a total of 470 (1–1) events.

Topology (1–3)

To be considered as a candidate (1–3) event the following cuts had to be satisfied:

(2a) exactly four reconstructed charged tracks should be seen in the event, where each track satisfied: (i) $d_0 < 2.0$ cm, (ii) $|z| < 10.0$ cm and (iii) $p_{xy} > 0.1$ GeV/c, where p_{xy} is the momentum component perpendicular to the beam line,

(2b) the event satisfied the coplanarity trigger,

(2c) the summed charge satisfied $\sum Q = 0$,

(2d) the summed charged track momentum satisfied $\sum p > 5.0$ GeV/c,

(2e) the tracks satisfied the following topological requirements: (i) one track (lone) was separated from each of the other three by $\alpha_{\text{lone}} > 90^\circ$ ($W < 25$ GeV) or $\alpha_{\text{lone}} > 120^\circ$ ($W > 25$ GeV) and (ii) within the three other tracks (3-track system) the angular separation of any pair did not exceed 90° , 60° , 45° for $W < 15$, $15 < W < 25$, $W > 25$ GeV respectively,

(2f) the lone particle momentum satisfied $p > 0.82$, 1.29, 2.0 GeV/c for $W < 15$, $15 < W < 25$, $W > 25$ GeV respectively,

(2g) the polar angle, θ , of the lone particle satisfied $|\cos \theta| < 0.8$,

(2h) the invariant mass, M_{+-} , of all pairs of oppositely charged tracks within the 3-track system, when assigned electron masses, satisfied $M_{+-} > 150$ MeV,

(2i) the radial distance, r , from the beam line to the intersection point of track pairs in (2h) satisfied $r < 6.0$ cm and

(2j) the invariant mass of the 3-track system, M_3 , considering all particles to be pions, satisfied $M_3 < 2.0$ GeV.

Cuts (2h) and (2i) reduce background from radiating Bhabha scattering events, (2e) and (2j) re-

duce background from single photon hadron production. As in the case of the (1–1) selection, 21 events which failed due to back-scattering in the coil were retained, resulting in a total of 350 (1–3) events.

Topology (3–3)

To be considered as a candidate (3–3) event the following cuts had to be satisfied:

(3a) exactly six reconstructed charged tracks should be seen in the event, where each track satisfied: (i) $d_0 < 2.0$ cm, (ii) $|z| < 10.0$ cm and (iii) $p_{xy} > 0.1$ GeV/c,

(3b) the event satisfied the coplanarity trigger,

(3c) the summed charge satisfied $\sum Q = 0$,

(3d) the summed charged track momentum satisfied $\sum p > 6.0$ GeV/c,

(3e) the tracks satisfied the following topological requirements: (i) two groups of three tracks were present and within each group the angular separation of any two tracks did not exceed 45° , (ii) the summed momentum vector of one 3-track system was separated by at least 90° from that of the other,

(3f) the polar angle of at least one of the summed momentum vectors satisfied $|\cos \theta| < 0.8$,

(3g) the invariant mass, M_{+-} , of all pairs of oppositely charged tracks within a 3-track system, when assigned electron masses, satisfied $M_{+-} > 150$ MeV,

(3h) the radial distance, r , from the beam axis to the intersection point of track pairs in (3g) satisfied $r < 6.0$ cm and

(3i) the invariant mass of each 3-track system, M_3 , considering all particles to be pions, satisfied $M_3 < 2.0$ GeV.

Cuts (3g) and (3h) reduce background from radiating Bhabha scattering events, (3e) and (3i) reduce background from single photon hadron production. Two events which failed due to back-scattering in the coil were retained, resulting in a total of 36 (3–3) events.

Topology (1–5)

To be considered as a candidate (1–5) event the following cuts were required to be satisfied:

(4a) exactly six reconstructed charged tracks should be seen in the event, where each track satisfied: (i) $d_0 < 2.0$ cm, (ii) $|z| < 10.0$ cm and (iii) $p_{xy} > 0.1$ GeV/c,

(4b) the event satisfied the coplanarity trigger,

(4c) the summed charge satisfied $\sum Q = 0$,

(4d) the summed charged track momentum satisfied $\sum p > 5.0$ GeV/c,

(4e) the tracks satisfied the following topological requirements: (i) one track (lone) was separated from each of the other five by $\alpha_{\text{lone}} > 120^\circ$ and (ii) within the five other tracks the angular separation of any pair did not exceed 60° ,

(4f) the lone particle momentum satisfied $p > 2.0 \text{ GeV}/c$,

(4g) the polar angle of the lone particle satisfied $|\cos \theta| < 0.8$,

(4h) the invariant mass, M_{+-} , of all pairs of oppositely charged tracks within the 5-track system, when assigned electron masses, satisfied $M_{+-} > 150 \text{ MeV}$,

(4i) the radial distance, r , from the beam line to the intersection point of track pairs in (4h) satisfied $r < 6.0 \text{ cm}$ and

(4j) the invariant mass of the 5-track system, M_5 , considering all particles to be pions, satisfied $M_5 < 2.0 \text{ GeV}$.

No candidate for the (1–5) category survived these requirements. As for previous categories, events failing due to back-scattering in the coil were searched for and none were found.

Appendix B. Particle Identification

When inside the particle identification acceptance of the electromagnetic calorimeters and/or the muon chambers, the events of categories (1–1) and (1–3) were subdivided according to the identity of the lone track as described below.

(a) Muon

If the track when projected into the muon chamber was associated with muon chamber hits with a muon confidence level $> 1\%$, then the track was considered to be a muon. Once identified as a muon then no further classification was attempted.

(b) Electron

To be identified as an electron within the LABC acceptance the following requirements were made:

(1) the track projected to within 2.0° of the centroid of an energy cluster deposited in the calorimeter,

(2) no other cluster was within 45° , subtended from the interaction point, of the cluster in (1),

(3) the track momentum, p , measured in the central detector matched the cluster energy, E , according to the relationship:

$$1.04 p - 2.5 \sigma < E < 1.04 p + 2.5 \sigma \quad (1)$$

where:

$$\sigma = (\sigma_E^2 + \sigma_p^2)^{\frac{1}{2}}$$

$$\sigma_p = 0.017 p^2$$

$$\sigma_E = 0.16 E^{\frac{1}{2}} + 0.03 E \text{ for } p < 4.1 \text{ and}$$

$$\sigma_E = 0.11 E \text{ for } p > 4.1 \text{ GeV}/c$$

where E is measured in units of GeV.

(4) the ratio, R , of the energy deposited in the front towers (6.1 radiation lengths) to that deposited in the back towers (7.6 r.l.) of the calorimeter satisfied $1/(0.65 + 0.1 p) < R < 10$

(5) the total number, N_s , of the orthogonal position measurement strips satisfied $N_s > 4(5)$ for $p < 5 (> 5) \text{ GeV}/c$

To be identified as an electron within the HASC acceptance the following requirements were made:

(1) the track projected to within 5.0° of the centroid of an energy cluster deposited in the calorimeter,

(2) no other cluster was within 45° , subtended from the interaction point, of the cluster in (1) and

(3) the track momentum, p , measured in the central detector matched the cluster energy, E , according to Eq. (1) with

$$\sigma_E = 0.29 E^{\frac{1}{2}} \text{ for } p < 3.7 \text{ and}$$

$$\sigma_E = 0.15 E \text{ for } p > 3.7 \text{ GeV}/c.$$

(c) Hadron

A track having an associated energy cluster in the electromagnetic calorimeters, but not identified as a muon or electron was called a hadron.

Tracks which were not identified as muons and had no associated energy clusters were not classified. This identification loss within the LABC and HASC acceptance was small, 2–3% per track, and was accounted for in the acceptance calculations.

References

- MARK II Collab. C.A. Blocker et al.: Phys. Rev. Lett. **49**, 1369 (1982); CELLO Collab. H.J. Behrend et al.: Phys. Lett. **114B**, 282 (1982); CELLO Collab. H.J. Behrend et al.: Z. Phys. C – Particles and Fields **23**, 103 (1984)
- TASSO Collab. R. Brandelik et al.: Phys. Lett. **113B**, 261 (1979); TASSO Collab. R. Brandelik et al.: Z. Phys. **C4**, 87 (1980)
- H. Boerner et al.: Nucl. Instrum. Methods **176** 151 (1980)
- TASSO Collab. R. Brandelik et al.: Phys. Lett. **108B**, 71 (1982)
- TASSO Collab. R. Brandelik et al.: Phys. Lett. **92B**, 199 (1980); T. Wyatt: D. Phil Thesis Oxford 1983, RAL Report HEP T 110
- I.C. Brock: D. Phil Thesis Oxford 1983, RAL Report HEP T 106

7. P.H. Daverveldt, R. Kleiss: contributed paper to the 5th International Colloquium on Computational Physics. Lecture Notes in Physics Vol. 191, Berlin, Heidelberg, New York: Springer 1983
8. J.A.M. Vermaseren: Talk at Intern. Workshop on $\gamma\gamma$ Collisions (Amiens), Lecture Notes in Physics, Vol. 134. Berlin, Heidelberg, New York: Springer 1980
9. B. Andersson, G. Gustafson, T. Sjostrand: Phys. Lett. **94B**, 211 (1980)
10. Y.-S. Tsai: Phys. Rev. **D4**, 2821 (1971)
11. F.A. Berends, R. Kleiss: Nucl. Phys. **B177**, 237 (1981)
12. TASSO Collab. R. Brandelik et al.: Phys. Lett. **94B**, 259 (1980)
13. P. Grossmann: OUNPL 74/83; H. Fesefeldt: Aachen PITHA Report, in preparation
14. MARK J Collab.: MIT Nucl. Sci. Rep. **131**, 4–23 (1983); B. Naroska: Int. Symp. on Lepton and Photon Interactions, Ithaca, p. 96, (1983); D.H. Saxon: Invited talk, Physics in Collisions IV, Santa Cruz (1984)
15. TASSO Collab. R. Brandelik et al.: Phys. Lett. **110B**, 173 (1982)
16. S.L. Glashow: Nucl. Phys. **22**, 579 (1961); S. Weinberg: Phys. Rev. Lett. **19**, 1264 (1967); A. Salam: Proc. 8th Nobel Symp., p. 367. Ed. N. Svartholm. Stockholm: Almqvist and Wiksell, 1968
17. R. Budny: Phys. Lett. **55B**, 227 (1975)
18. F.A. Berends, K.J.F. Gaemers, R. Gastmans: Nucl. Phys. **B63**, 381 (1973); F.A. Berends, R. Gastmans: private communication
19. A. Boehm: Aachen PITHA report, PITHA 84/13
20. Particle Data Group: Rev. Mod. Phys. **52**, No. 2, Part II (1980)
21. UA1 Collab. G. Arnison et al.: Phys. Lett. **126B**, 398 (1983); UA2 Collab. P. Bagnaia et al.: Phys. Lett. **129B**, 130 (1983)
22. W. Krenz: Aachen PITHA Report, PITHA 82/26